AIMS Mathematics, 9(12): 34886–34905.
DOI: 10.3934/math.20241661
Received: 29 October 2024
Revised: 28 November 2024
Accepted: 29 November 2024
Published: 13 December 2024

https://www.aimspress.com/journal/Math

Research article

Probing the diversity of kink solitons in nonlinear generalised Zakharov-Kuznetsov-Benjamin-Bona-Mahony dynamical model

Naher Mohammed A. Alsafri[1,*] **and Hamad Zogan**[2]

[1] Department of Mathematics, Faculty of Science, University of Jeddah, Saudi Arabia
[2] Department of Computer Science, College of Engineering and Computer Science, Jazan University, Jazan, Kingdom of Saudi Arabia

* **Correspondence:** Email: nmalsafri@uj.edu.sa.

Abstract: This investigation offers an innovative analytical strategy, namely the Riccati modified extended simple equation method (RMESEM), to establish and analyze soliton results of the (2+1)-dimensional dynamical generalized Zakharov-Kuznetsov-Benjamin-Bona-Mahony equation (GZK-BBME) in plasma physics. This equation models the physical phenomena of long waves with small and finite amplitude in magnetic plasma. Using a wave transformation, the employed transformative technique first converts GZK-BBME to a nonlinear ordinary differential equation (NODE). With the incorporation of the Riccati equation, a close-form solution is then assumed for the resultant NODE by RMESEM, which converts the NODE into a set of algebraic equations. The fresh plethora of soliton results in the form of rational, exponential, rational-hyperbolic and periodic functional cases are obtained by addressing this set of equations. Several contour, 3D, and 2D graphs are also employed to visualizes the dynamics of these constructed soliton results. These graphs demonstrate that the acquired solitons adopts the type of diverse kink solitons, including cuspon, dark, bright, lump-type, and dark-bright kinks. In addition, our proposed RMESEM shows the applications of the model by producing different traveling soliton results, providing qualitative information on the GZK-BBMEs and possible applications in dealing with other similar kinds of non-linear models.

Keywords: Riccati modified extended simple equation method; dynamical systems; generalized Zakharov-Kuznetsov-Benjamin-Bona-Mahony equation; Riccati equation; kink solitons
Mathematics Subject Classification: 34G20, 35A20, 35A22, 35R11

1. Introduction

Nonlinear partial differential equations (NPDEs) are crucial due to their ability to decode a wide-ranging of phenomena, as well as wave bending, fluid mechanics, hydrodynamics, organic molecular

dispersion, magnetism, thermal conductivity, and many more. These phenomena are found across multiple scientific areas, such as mathematics, physics, engineering, biology, and finance. The broad range of NLPDEs is shown by a variety of equations, such as the Higgs system, advection equation, Boussinesq equation, Fisher's equation, and Burger's equation, among others [1–5].

Several asymptotic methods have been proposed in other studies to explore the internal dynamic behaviors of nonlinear partial differential equations (NPDEs) and fractional NPDEs with investigations on propagating solitons and other travelling wave solutions [6–10]. A soliton is an auto-oscillating wave-packet that preserves both its shape and speed during its propagation due to the fine-tuning between dispersion and nonlinearity. Kink waves, shock waves, lump waves, damped waves, periodic waves, etc are a few examples of solitons are present, which are described by soliton theory [11–13]. Despite the abundant availability of numerical solutions, analysts often resort to analytical methods because of the ability to explain the flow of physics and the accuracy of estimate of the behaviors of the system [14–16]. As a result, work on developing analytical treatments to investigate the solitonic behavior of NPDEs and fractional NPDEs is still ongoing, and several analytical methods have been created to investigate soliton solutions. F-expansion technique [17], sech-tanh technique [18], Sardar sub-equation technique [19], (G'/G)-expansion technique [20–23], exp-function technique [24], sub-equation technique [25], tanh technique [26], (G'/G^2)-expansion technique [27], Hirota bilinear technique [28], Kudryashov technique [29], Poincaré-Lighthill Kuo approach [30], unified technique [31], Riccati-Bernoulli Sub-ODE technique [32], extended direct algebraic technique [33–37], auxiliary equation method [38], simple equation method [39], and RMESEM [40] are a few of these methods.

To discover cases of propagating solitons and other traveling waves, results for NPDEs and NFPDEs, this work establishes a new modification in a novel analytical technique called RMESEM with extended Riccati equation. This approach uses a variable-form wave transformation to transform the NPDE or NFPDE into an integer-order NODE. The resulting NODE is considered to have a series-based result (incorporating the solution of the Riccati equation). The substitution of the supposed solution in the resultant NODE transforms it into a set of algebraic equations. The soliton solutions for the relevant NPDEs and NFPDEs are acquired by more thoroughly finding the solutions of algebraic equations. The families of soliton solutions produced by RMESEM with the extended Riccati equation can help us comprehend the fundamental physical mechanisms and behavioral patterns of the nonlinear system.

To showcase the effectiveness of the improved RMESEM, the method is utilized to acquire soliton solutions for the (2+1)-dimensional GZK-BBME. In 1972, Benjamin et al. [41] investigated the issue of long waves with small and finite amplitudes and put out the Benjamin-Bona-Mahony equation (BBME), which took the following form:

$$v_t + \alpha v_x + \beta v v_x - \gamma v_{txx} = 0. \tag{1.1}$$

To study weakly nonlinear ion-acoustic oscillations in low-pressure magnetized plasma, Zakharov and Kuznetsov [42] extended the Korteweg-de Vries (KdV) equation, resulting in the formulation of the Zakharov-Kuznetsov equation (ZKE) as:

$$v_t + \alpha v v_x + (v_{xx} + v_{yy} + v_{zz})_x = 0, \tag{1.2}$$

where v denotes ion velocity with the magnetic fields and is non-dimensional. Wazwaz [43] merged

the ZKE and BBME equations in 2005 to create the (2+1) dimensional GZK-BBM equation [40]:

$$v_t + v_x + \alpha(v^\delta)_x + \beta(v_{xt} + v_{yy})_x = 0, \quad \delta > 1, \tag{1.3}$$

where $v = v(t, x, y)$, the coefficients α and β are the relative dispersion and nonlinear parameters respectively, and x and y are the propagating & transverse coordinates. The nonlinear influence is introduced into the equation by the term $(v^\delta)_x$. This formula is applied to the ZK-model analysis of long waves with finite amplitude. This equation's odd-order derivatives, v_{xxt} and v_{yyx}, take the dispersion effect into account. Examining the way the nonlinear and dispersion effects interact with the problem is one goal of the generalized GZK-BBME investigation. For instance, the tanh and sine-cosine approach was used to solve (3) [44]. By using a modified simple equation approach, Khan et al. [45] were able to get solitary wave solutions to the GZK-BBME for $n = 3$. In 2015, Guner et al. [46] revealed the dark and bright soliton solution of the GZK-BBME. Finally, Patel and Kumar acquired numerical and semi-analytical solutions for GZK-BBME for $n = 2$ and $n = 3$ by the Adomian decomposition method and the variational iteration method, respectively, under some initial conditions [40]. The remaining task of the present analysis is to constructs and examine the propagation of the solitons in the context of GZK-BBME for $n = 3$ articulated in (2.1).

The rest of the study is structured as follows: In Section 2, we detail the working process of RMESEM. Following this approach, we develop soliton solutions for the GZK-BBME in Section 3. The depictions and graphical discussion are presented in Section 4. Lastly, Section 5 provides the conclusion in our research proposal.

2. The operational methodology of RMESEM

This section outlines the operational mechanism of RMESEM for constructing soliton solutions for NPDEs. Suppose the following general NPDE:

$$P(v, v_t, v_x, v_y, vv_t, \ldots) = 0, \tag{2.1}$$

where $v = v(t, x, y)$ is an unknown function, P is the polynomial of $v(t, x, y)$, while the subscripts signify partial derivatives.

The main steps of the proposed RMESEM are as follows:

Step 1. Take into consideration the ensuing wave transformation

$$v(t, x, y) = V(\zeta), \quad \text{where} \quad \zeta = x + y - \omega t, \tag{2.2}$$

where ω denotes wave speed. Equation (2.1) is converted into the following NODE using the above wave transformation:

$$Q(V, V'V, V', \ldots) = 0, \tag{2.3}$$

where the primes indicate the ordinary derivatives of V with respect to ζ, and Q is a polynomial of V and its derivatives.

Step 2. Equation (2.3) is sometimes integrated term by term to be made conformable for the homogeneous balancing rule.

Step 3. Following that, we suppose that a closed-form wave solution for Eq (2.3) can be expressed in the ensuing form:

$$V(\zeta) = \sum_{j=0}^{\gamma} k_j \left(\frac{\Phi'(\zeta)}{\Phi(\zeta)}\right)^j + \sum_{\epsilon=0}^{\gamma-1} s_\epsilon \left(\frac{\Phi'(\zeta)}{\Phi(\zeta)}\right)^\epsilon \cdot \left(\frac{1}{\Phi(\zeta)}\right), \tag{2.4}$$

where $k_j (j = 0, ..., \gamma)$ and $s_\epsilon (\epsilon = 0, ..., \gamma-1)$ represent the unknown constants that need to be determined later and $\Phi(\zeta)$ satisfies the subsequent 1st order Riccati equation:

$$\Phi'(\zeta) = p + q\Phi(\zeta) + r(\Phi(\zeta))^2, \tag{2.5}$$

where p, q and r are constants.

Step 4. To calculate the integer γ presented in Eq (2.4), we take the homogeneous balance between the highest nonlinear term and the highest-order derivative term in Eq (2.3).

Step 5. Substituting the value of γ got in step 4 into Eq (2.4) and substituting the result together with $\Phi(\zeta)$ raised to the exponent equal to the index of the integral on the left-hand side of Eq (2.3) or substituting the result with $\Phi(\zeta)$ when we have integrated Eq (2.3) gives an expression in terms of $\Phi(\zeta)$. New additional construction by comparison of coefficient expression gives a system of algebraic equations of $k_j (j = 0, ..., \gamma)$ and $s_\epsilon (\epsilon = 0, ..., \gamma-1)$ with other associated parameters that are introduced.

Step 6. Solving the algebraic system obtained in Step 5 with the help of algebraic software Maple yields values of $k_j (j = 0, ..., \gamma)$ and $s_\epsilon (\epsilon = 0, ..., \gamma - 1)$ with additional associated parameters.

Step 7. Finally, soliton solutions to Eq (2.1) are derived by determining and substituting the calculated values of parameters in Eq (2.4) with the solutions of Eq (2.5) that are given in Table 1.

3. Execution of RMESEM

This section employs the proposed RMESEM for the establishment of new plethora of soliton solutions for GZK-BBME with $\delta = 3$ of the form:

$$v_t + v_x + \alpha(v^3)_x + \beta(v_{xt} + v_{yy})_x = 0. \tag{3.1}$$

We proceed by performing the wave transformation given in Eq (2.2), which transforms Eq (3.1) into the ensuing NODE:

$$-\omega V' + V' + \alpha(V^3)' + \beta(-\omega V'' + V'')' = 0. \tag{3.2}$$

Upon integrating Eq (3.2) with zero constant of integration, we obtain the following NODE:

$$(1 - \omega)V + \alpha V^3 + (1 - \omega)\beta V''. \tag{3.3}$$

Establishing the principle of homogenous balance between terms V'' and V^3 in Eq (3.3) suggests that $2+\gamma = 3\gamma$ which applies $\gamma = 1$. Substituting $\gamma = 1$ in Eq (2.4) presents the series form closed solutions for Eq (3.3):

$$V(\zeta) = \sum_{j=0}^{1} k_j \left(\frac{\Phi'(\zeta)}{\Phi(\zeta)}\right)^j + \left(\frac{s_0}{\Phi(\zeta)}\right). \tag{3.4}$$

Table 1. The solutions $\Phi(\zeta)$ that meet the particular Riccati equation in (2.4) and the structure of $\left(\frac{\Phi'(\zeta)}{\Phi(\zeta)}\right)$, where $\kappa = q^2 - 4rp$ and $\wp = \cosh\left(\frac{1}{4}\sqrt{\kappa}\zeta\right)\sinh\left(\frac{1}{4}\sqrt{\kappa}\zeta\right)$.

S. No.	Family	Condition(s)	$\Phi(\zeta)$	$\left(\frac{\Phi'(\zeta)}{\Phi(\zeta)}\right)$
1	Trigonometric Solutions	$\kappa < 0, \quad r \neq 0$	$-\frac{q}{2r} + \frac{\sqrt{-\kappa}\tan\left(\frac{1}{2}\sqrt{-\kappa}\zeta\right)}{2r}$,	$-\frac{1}{2}\frac{\kappa\left(1+\left(\tan\left(\frac{1}{2}\sqrt{-\kappa}\zeta\right)\right)^2\right)}{-q+\sqrt{-\kappa}\tan\left(\frac{1}{2}\sqrt{-\kappa}\zeta\right)}$,
			$-\frac{q}{2r} - \frac{\sqrt{-\kappa}\cot\left(\frac{1}{2}\sqrt{-\kappa}\zeta\right)}{2r}$,	$\frac{1}{2}\frac{\left(1+\left(\cot\left(\frac{1}{2}\sqrt{-\kappa}\zeta\right)\right)^2\right)\kappa}{q+\sqrt{-\kappa}\cot\left(\frac{1}{2}\sqrt{-\kappa}\zeta\right)}$,
			$-\frac{q}{2r} + \frac{\sqrt{-\kappa}\left(\tan\left(\sqrt{-\kappa}\zeta\right)+\left(\sec\left(\sqrt{-\kappa}\zeta\right)\right)\right)}{2r}$,	$-\frac{\kappa\left(1+\sin\left(\sqrt{-\kappa}\zeta\right)\right)\sec\left(\sqrt{-\kappa}\zeta\right)}{-q\cos\left(\sqrt{-\kappa}\zeta\right)+\sqrt{-\kappa}\sin\left(\sqrt{-\kappa}\zeta\right)+\sqrt{-\kappa}}$,
			$-\frac{q}{2r} + \frac{\sqrt{-\kappa}\left(\tan\left(\sqrt{-\kappa}\zeta\right)-\left(\sec\left(\sqrt{-\kappa}\zeta\right)\right)\right)}{2r}$.	$\frac{\kappa\left(\sin\left(\sqrt{-\kappa}\zeta\right)-1\right)\sec\left(\sqrt{-\kappa}\zeta\right)}{-q\cos\left(\sqrt{-\kappa}\zeta\right)+\sqrt{-\kappa}\sin\left(\sqrt{-\kappa}\zeta\right)-\sqrt{-\kappa}}$.
2	Rational Solutions	$\kappa = 0$	$-2\frac{p(q\zeta+2)}{q^2\zeta}$,	$-2\frac{1}{\zeta(q\zeta+2)}$,
		$\kappa = 0, \& \ q = r = 0$	ζp,	$\frac{1}{\zeta}$,
		$\kappa = 0, \& \ q = p = 0$	$-\frac{1}{\zeta r}$.	$-\frac{1}{\zeta}$.
3	Hyperbolic Solutions	$\kappa > 0, \quad r \neq 0$	$-\frac{q}{2r} - \frac{\sqrt{\kappa}\tanh\left(\frac{1}{2}\sqrt{\kappa}\zeta\right)}{2r}$,	$-\frac{1}{2}\frac{\left(-1+\left(\tanh\left(\frac{1}{2}\sqrt{\kappa}\zeta\right)\right)^2\right)\kappa}{q+\sqrt{\kappa}\tanh\left(\frac{1}{2}\sqrt{\kappa}\zeta\right)}$,
			$-\frac{q}{2r} - \frac{\sqrt{\kappa}\left(\tanh\left(\sqrt{\kappa}\zeta\right)+i\left(\operatorname{sech}\left(\sqrt{\kappa}\zeta\right)\right)\right)}{2r}$,	$-\frac{\kappa\left(-1+i\sinh\left(\sqrt{\kappa}\zeta\right)\right)}{\cosh\left(\sqrt{\kappa}\zeta\right)\left(q\cosh\left(\sqrt{\kappa}\zeta\right)+\sqrt{\kappa}\sinh\left(\sqrt{\kappa}\zeta\right)+i\sqrt{\kappa}\right)}$,
			$-\frac{q}{2r} - \frac{\sqrt{\kappa}\left(\tanh\left(\sqrt{\kappa}\zeta\right)-i\left(\operatorname{sech}\left(\sqrt{\kappa}\zeta\right)\right)\right)}{2r}$,	$-\frac{\kappa\left(1+i\sinh\left(\sqrt{\kappa}\zeta\right)\right)}{\cosh\left(\sqrt{\kappa}\zeta\right)\left(-q\cosh\left(\sqrt{\kappa}\zeta\right)-\sqrt{\kappa}\sinh\left(\sqrt{\kappa}\zeta\right)+i\sqrt{\kappa}\right)}$,
			$-\frac{q}{2r} - \frac{\sqrt{\kappa}\left(\coth\left(\sqrt{\kappa}\zeta\right)+\left(\operatorname{csch}\left(\sqrt{\kappa}\zeta\right)\right)\right)}{2r}$.	$-\frac{1}{4}\frac{\kappa\left(2\left(\cosh\left(\frac{1}{4}\sqrt{\kappa}\zeta\right)\right)^2-1\right)}{\wp\left(-2q\wp+\sqrt{\kappa}\right)}$.
4	Rational-Hyperbolic Solutions	$p = 0, \& \ q \neq 0, r \neq 0$	$-\frac{\lambda b}{r(\cosh(b\zeta)-\sinh(b\zeta)+\lambda)}$,	$\frac{q(\sinh(q\zeta)-\cosh(q\zeta))}{-\cosh(q\zeta)+\sinh(q\zeta)-\lambda}$,
			$-\frac{b(\cosh(b\zeta)+\sinh(b\zeta))}{r(\cosh(b\zeta)+\sinh(b\zeta)+\mu)}$.	$\frac{q\mu}{\cosh(q\zeta)+\sinh(q\zeta)+\mu}$.
5	Exponential Solutions	$r = 0, \& \ q = \Upsilon, p = h\Upsilon$	$e^{\Upsilon\zeta} - h$,	$\frac{\Upsilon e^{\Upsilon\zeta}}{e^{\Upsilon\zeta}-h}$,
		$p = 0, \& \ q = \Upsilon, r = h\Upsilon$	$\frac{e^{\Upsilon\zeta}}{1-he^{\Upsilon\zeta}}$.	$-\frac{\Upsilon}{-1+he^{\Upsilon\zeta}}$.

An expression in $\Phi(\zeta)$ is generated by entering Eq (3.4) into Eq (3.3) and gathering all terms with the equal exponents of $\Phi(\zeta)$. The achieved expressions can be reduced to the ensuing scheme of seven nonlinear algebraic equations by putting the coefficients to zero:

$$2\beta k_1 r^3 - 2\beta\omega k_1 r^3 + \alpha {k_1}^3 r^3 = 0,$$

$$3\alpha {k_1}^3 q r^2 - 3\beta\omega k_1 q r^2 + 3\alpha k_0 {k_1}^2 r^2 + 3\beta k_1 q r^2 = 0,$$

$$\begin{aligned}&-2\beta\omega k_1 r^2 p + 2\beta k_1 r^2 p + 3\alpha {k_0}^2 k_1 r - \beta\omega k_1 q^2 r + 3\alpha {k_1}^3 p r^2\\ &-\omega k_1 r + k_1 r + 3\alpha {k_1}^3 q^2 r + 6\alpha k_0 {k_1}^2 q r + \beta k_1 q^2 r + 3\alpha {k_1}^2 r^2 s_0 = 0,\end{aligned}$$

$$\begin{aligned}&6\alpha {k_1}^3 p q r + \alpha {k_0}^3 + 2\beta k_1 q p r + 6\alpha k_0 k_1 r s_0 + k_1 q - \omega k_1 q + 6\alpha k_0 {k_1}^2 p r + 3\alpha {k_0}^2 k_1 q\\ &+ 6\alpha {k_1}^2 q r s_0 + k_0 + \beta s_0 q r - \beta\omega s_0 q r + \alpha {k_1}^3 q^3 + 3\alpha k_0 {k_1}^2 q^2 - \omega k_0 - 2\beta\omega k_1 q p r = 0,\end{aligned}$$

$$-\omega s_0+\beta s_0q^2+6\alpha {k_1}^2prs_0+6\alpha k_0{k_1}^2pq+3\alpha {k_1}^3p^2r-\omega k_1p+k_1p+3\alpha {k_0}^2s_0$$
$$-2\beta\omega k_1rp^2+s_0-2\beta\omega s_0pr+6\alpha k_0k_1qs_0+3\alpha {k_0}^2k_1p+2\beta s_0pr+\beta k_1q^2p$$
$$+3\alpha k_1{s_0}^2+3\alpha {k_1}^3pq^2-\beta\omega s_0q^2+3\alpha {k_1}^2q^2s_0+2\beta k_1rp^2-\beta\omega k_1q^2p=0,$$
$$3\alpha {k_1}^3p^2q+3\beta s_0pq+3\alpha k_1q{s_0}^2-3\beta\omega s_0pq+6\alpha k_0k_1ps_0$$
$$-3\beta\omega k_1qp^2+6\alpha {k_1}^2pqs_0+3\alpha k_0{k_1}^2p^2+3\beta k_1qp^2+3\alpha k_0{s_0}^2=0,$$

and

$$-2\beta\omega s_0p^2+\alpha {k_1}^3p^3+3\alpha {k_1}^2p^2s_0+\alpha {s_0}^3-2\beta\omega k_1p^3+2\beta s_0p^2+3\alpha k_1p{s_0}^2+2\beta k_1p^3=0.$$

When tackling the result scheme with Maple, the followings three sorts of results become available:

Case 1.

$$k_1=0,\ \ s_0=s_0,\ \ k_0=\frac{1}{2}\frac{s_0q}{p},\ \ \beta=\frac{2}{\kappa},\ \ \alpha=4\frac{p^2(\omega-1)}{\kappa\,{s_0}^2},\ \ \omega=\omega. \tag{3.5}$$

Case 2.

$$k_1=k_1,\ \ s_0=s_0,\ \ k_0=k_0,\ \ \beta=\beta,\ \ \alpha=0,\ \ \omega=1. \tag{3.6}$$

Case 3.

$$k_1=k_1,\ \ s_0=-k_1p,\ \ k_0=-\frac{1}{2}k_1q,\ \ \beta=\frac{2}{\kappa},\ \ \alpha=4\frac{\omega-1}{\kappa\,{k_1}^2},\ \ \omega=\omega. \tag{3.7}$$

When Case 1 is assumed and Eqs (2.2) and (3.4), together with the consistent general result of Eq (2.5) given in Table 1. The following cases of soliton results for GZK-BBME expressed in Eq (3.1) result:

Set. 1.1. With $\kappa<0,\ r\neq0,$

$$v_{1,1}(x,y,t)=\frac{1}{2}\frac{s_0q}{p}+s_0\left(-\frac{1}{2}\frac{q}{r}+\frac{1}{2}\frac{\sqrt{-\kappa}\tan\left(\frac{1}{2}\sqrt{-\kappa}\zeta\right)}{r}\right)^{-1}, \tag{3.8}$$

$$v_{1,2}(x,y,t)=\frac{1}{2}\frac{s_0q}{p}+s_0\left(-\frac{1}{2}\frac{q}{r}-\frac{1}{2}\frac{\sqrt{-\kappa}\cot\left(\frac{1}{2}\sqrt{-\kappa}\zeta\right)}{r}\right)^{-1}, \tag{3.9}$$

$$v_{1,3}(x,y,t)=\frac{1}{2}\frac{s_0q}{p}+s_0\left(-\frac{1}{2}\frac{q}{r}+\frac{1}{2}\frac{\sqrt{-\kappa}\left(\tan\left(\sqrt{-\kappa}\zeta\right)+\sec\left(\sqrt{-\kappa}\zeta\right)\right)}{r}\right)^{-1}, \tag{3.10}$$

and

$$v_{1,4}(x,y,t)=\frac{1}{2}\frac{s_0q}{p}+s_0\left(-\frac{1}{2}\frac{q}{r}+\frac{1}{2}\frac{\sqrt{-\kappa}\left(\tan\left(\sqrt{-\kappa}\zeta\right)-\sec\left(\sqrt{-\kappa}\zeta\right)\right)}{r}\right)^{-1}. \tag{3.11}$$

Set. 1.2. With $\kappa > 0,\ r \neq 0$,

$$v_{1,5}(x,y,t) = \frac{1}{2}\frac{s_0 q}{p} + s_0\left(-\frac{1}{2}\frac{q}{r} - \frac{1}{2}\frac{\sqrt{\kappa}\tanh\left(\frac{1}{2}\sqrt{\kappa}\zeta\right)}{r}\right)^{-1}, \tag{3.12}$$

$$v_{1,6}(x,y,t) = \frac{1}{2}\frac{s_0 q}{p} + s_0\left(-\frac{1}{2}\frac{q}{r} - \frac{1}{2}\frac{\sqrt{\kappa}\left(\tanh\left(\sqrt{\kappa}\zeta\right) + i\,\mathrm{sech}\left(\sqrt{\kappa}\zeta\right)\right)}{r}\right)^{-1}, \tag{3.13}$$

$$v_{1,7}(x,y,t) = \frac{1}{2}\frac{s_0 q}{p} + s_0\left(-\frac{1}{2}\frac{q}{r} - \frac{1}{2}\frac{\sqrt{\kappa}\left(\tanh\left(\sqrt{\kappa}\zeta\right) - i\,\mathrm{sech}\left(\sqrt{\kappa}\zeta\right)\right)}{r}\right)^{-1}, \tag{3.14}$$

and

$$v_{1,8}(x,y,t) = \frac{1}{2}\frac{s_0 q}{p} + s_0\left(-\frac{1}{2}\frac{q}{r} - \frac{1}{4}\frac{\sqrt{\kappa}\left(\tanh\left(\frac{1}{4}\sqrt{\kappa}\zeta\right) - \coth\left(\frac{1}{4}\sqrt{\kappa}\zeta\right)\right)}{r}\right)^{-1}. \tag{3.15}$$

Set. 1.3. With $q = \Upsilon$, $p = h\Upsilon (h \neq 0)$ and $r = 0$,

$$v_{1,9}(x,y,t) = \frac{1}{2}\frac{s_0}{h} + \frac{s_0}{\mathrm{e}^{\Upsilon\zeta} - h}. \tag{3.16}$$

In above solutions $\zeta = x + y - \omega t$.

When Case 2 is assumed and Eqs (2.2) and (3.4) together with the consistent general result of Eq (2.5) given in Table 1. The following cases of soliton results for GZK-BBME expressed in Eq (3.1) result:

Set. 2.1. With $\kappa < 0,\ r \neq 0$,

$$v_{2,1}(x,y,t) = k_0 - \frac{1}{2}\frac{k_1\kappa\left(1 + \left(\tan\left(\frac{1}{2}\sqrt{-\kappa}\zeta\right)\right)^2\right)}{-q + \sqrt{-\kappa}\tan\left(\frac{1}{2}\sqrt{-\kappa}\zeta\right)} + s_0\left(-\frac{1}{2}\frac{q}{r} + \frac{1}{2}\frac{\sqrt{-\kappa}\tan\left(\frac{1}{2}\sqrt{-\kappa}\zeta\right)}{r}\right)^{-1}, \tag{3.17}$$

$$v_{2,2}(x,y,t) = k_0 + \frac{1}{2}\frac{k_1\kappa\left(1 + \left(\cot\left(\frac{1}{2}\sqrt{-\kappa}\zeta\right)\right)^2\right)}{q + \sqrt{-\kappa}\cot\left(\frac{1}{2}\sqrt{-\kappa}\zeta\right)} + s_0\left(-\frac{1}{2}\frac{q}{r} - \frac{1}{2}\frac{\sqrt{-\kappa}\cot\left(\frac{1}{2}\sqrt{-\kappa}\zeta\right)}{r}\right)^{-1}, \tag{3.18}$$

$$\begin{aligned} v_{2,3}(x,y,t) =& k_0 - \frac{k_1\kappa\left(1 + \sin\left(\sqrt{-\kappa}\zeta\right)\right)}{\cos\left(\sqrt{-\kappa}\zeta\right)\left(-q\cos\left(\sqrt{-\kappa}\zeta\right) + \sqrt{-\kappa}\sin\left(\sqrt{-\kappa}\zeta\right) + \sqrt{-\kappa}\right)} \\ &+ s_0\left(-\frac{1}{2}\frac{q}{r} + \frac{1}{2}\frac{\sqrt{-\kappa}\left(\tan\left(\sqrt{-\kappa}\zeta\right) + \sec\left(\sqrt{-\kappa}\zeta\right)\right)}{r}\right)^{-1} + k_0, \end{aligned} \tag{3.19}$$

and

$$\begin{aligned} v_{2,4}(x,y,t) =& \frac{k_1\kappa\left(\sin\left(\sqrt{-\kappa}\zeta\right) - 1\right)}{\cos\left(\sqrt{-\kappa}\zeta\right)\left(-q\cos\left(\sqrt{-\kappa}\zeta\right) + \sqrt{-\kappa}\sin\left(\sqrt{-\kappa}\zeta\right) - \sqrt{-\kappa}\right)} \\ &+ s_0\left(-\frac{1}{2}\frac{q}{r} + \frac{1}{2}\frac{\sqrt{-\kappa}\left(\tan\left(\sqrt{-\kappa}\zeta\right) - \sec\left(\sqrt{-\kappa}\zeta\right)\right)}{r}\right)^{-1} + k_0. \end{aligned} \tag{3.20}$$

Set. 2.2. With $\kappa > 0,\ r \neq 0$,

$$v_{2,5}(x,y,t) = k_0 - \frac{1}{2}\frac{k_1\kappa\left(-1+\left(\tanh\left(1/2\ \sqrt{\kappa}\zeta\right)\right)^2\right)}{q+\ \sqrt{\kappa}\tanh\left(\frac{1}{2}\ \sqrt{\kappa}\zeta\right)} + s_0\left(-\frac{1}{2}\frac{q}{r} - \frac{1}{2}\frac{\sqrt{\kappa}\tanh\left(\frac{1}{2}\ \sqrt{\kappa}\zeta\right)}{r}\right)^{-1}, \tag{3.21}$$

$$\begin{aligned} v_{2,6}(x,y,t) = &-\frac{k_1\kappa\left(-1+i\sinh\left(\sqrt{\kappa}\zeta\right)\right)}{\cosh\left(\sqrt{\kappa}\zeta\right)\left(q\cosh\left(\sqrt{\kappa}\zeta\right)+\ \sqrt{\kappa}\sinh\left(\sqrt{\kappa}\zeta\right)+i\sqrt{\kappa}\right)} \\ &+ s_0\left(-\frac{1}{2}\frac{q}{r} - \frac{1}{2}\frac{\sqrt{\kappa}\left(\tanh\left(\sqrt{\kappa}\zeta\right)+i\mathrm{sech}\left(\sqrt{\kappa}\zeta\right)\right)}{r}\right)^{-1} + k_0, \end{aligned} \tag{3.22}$$

$$\begin{aligned} v_{2,7}(x,y,t) = &-\frac{k_1\kappa\left(1+i\sinh\left(\sqrt{\kappa}\zeta\right)\right)}{\cosh\left(\sqrt{\kappa}\zeta\right)\left(-q\cosh\left(\sqrt{\kappa}\zeta\right)-\ \sqrt{\kappa}\sinh\left(\sqrt{\kappa}\zeta\right)+i\sqrt{\kappa}\right)} \\ &+ s_0\left(-\frac{1}{2}\frac{q}{r} - \frac{1}{2}\frac{\sqrt{\kappa}\left(\tanh\left(\sqrt{\kappa}\zeta\right)-i\mathrm{sech}\left(\sqrt{\kappa}\zeta\right)\right)}{r}\right)^{-1} + k_0, \end{aligned} \tag{3.23}$$

and

$$\begin{aligned} v_{2,8}(x,y,t) = &-\frac{1}{4}\frac{k_1\kappa\left(2\left(\cosh\left(\frac{1}{4}\sqrt{\kappa}\zeta\right)\right)^2-1\right)}{\cosh\left(\frac{1}{4}\sqrt{\kappa}\zeta\right)\sinh\left(\frac{1}{4}\ \sqrt{\kappa}\zeta\right)\left(-2\,q\cosh\left(\frac{1}{4}\ \sqrt{\kappa}\zeta\right)\sinh\left(\frac{1}{4}\ \sqrt{\kappa}\zeta\right)+\ \sqrt{\kappa}\right)} \\ &+ s_0\left(-\frac{1}{2}\frac{q}{r} - \frac{1}{4}\frac{\sqrt{\kappa}\left(\tanh\left(\frac{1}{4}\ \sqrt{\kappa}\zeta\right)-\coth\left(\frac{1}{4}\ \sqrt{\kappa}\zeta\right)\right)}{r}\right)^{-1} + k_0. \end{aligned} \tag{3.24}$$

Set. 2.3. With $\kappa = 0,\quad q \neq 0$,

$$v_{2,9}(x,y,t) = k_0 - 2\frac{k_1}{\zeta\ (q\zeta+2)} - \frac{1}{2}\frac{s_0q^2\zeta}{p\,(q\zeta+2)}. \tag{3.25}$$

Set. 2.4. With $\kappa = 0$, in case when $q = r = 0$,

$$v_{2,10}(x,y,t) = k_0 + \frac{k_1}{\zeta} + \frac{s_0}{p\zeta}. \tag{3.26}$$

Set. 2.5. With $\kappa = 0$, in case when $q = p = 0$,

$$v_{2,11}(x,y,t) = k_0 - \frac{k_1}{\zeta} - s_0r\zeta. \tag{3.27}$$

Set. 2.6. With $q = \Upsilon$, $p = h\Upsilon(h \neq 0)$ and $r = 0$,

$$v_{2,12}(x,y,t) = k_0 + \frac{k_1\Upsilon\,\mathrm{e}^{\Upsilon\zeta}}{\mathrm{e}^{\Upsilon\zeta}-h} + \frac{s_0}{\mathrm{e}^{\Upsilon\zeta}-h}. \tag{3.28}$$

Set. 2.7. With $q = \Upsilon$, $r = h\Upsilon(h \neq 0)$ and $p = 0$,

$$v_{2,13}(x,y,t) = k_0 - \frac{k_1\Upsilon}{-1 + h\mathrm{e}^{\Upsilon\zeta}} + \frac{s_0\left(1 - h\mathrm{e}^{\Upsilon\zeta}\right)}{\mathrm{e}^{\Upsilon\zeta}}. \tag{3.29}$$

Set. 2.8. With $p = 0$, $r \neq 0$ and $q \neq 0$,

$$v_{2,14}(x,y,t) = k_0 + \frac{k_1 q\left(\sinh(q\zeta) - \cosh(q\zeta)\right)}{-\cosh(q\zeta) + \sinh(q\zeta) - \lambda} - \frac{s_0 r\left(\cosh(q\zeta) - \sinh(q\zeta) + \lambda\right)}{\lambda q}, \tag{3.30}$$

and

$$v_{2,15}(x,y,t) = k_0 + \frac{k_1 q\mu}{\cosh(q\zeta) + \sinh(q\zeta) + \mu} - \frac{s_0 r\left(\cosh(q\zeta) + \sinh(q\zeta) + \mu\right)}{q\left(\cosh(q\zeta) + \sinh(q\zeta)\right)}. \tag{3.31}$$

In above solutions $\zeta = x + y - t$.

When Case 3 is assumed and Eqs (2.2) and (3.4) together with the consistent general result of Eq (2.5) given in Table 1. The following cases of soliton results for GZK-BBME expressed in Eq (3.1) result:

Set. 3.1. With $\kappa < 0,\ r \neq 0$,

$$v_{3,1}(x,y,t) = -\frac{1}{2}k_1 q - \frac{1}{2}\frac{k_1\kappa\left(1 + \left(\tan\left(\frac{1}{2}\sqrt{-\kappa}\zeta\right)\right)^2\right)}{-q + \sqrt{-\kappa}\tan\left(\frac{1}{2}\sqrt{-\kappa}\zeta\right)} - k_1 p\left(-\frac{1}{2}\frac{q}{r} + \frac{1}{2}\frac{\sqrt{-\kappa}\tan\left(\frac{1}{2}\sqrt{-\kappa}\zeta\right)}{r}\right)^{-1}, \tag{3.32}$$

$$v_{3,2}(x,y,t) = -\frac{1}{2}k_1 q + \frac{1}{2}\frac{k_1\kappa\left(1 + \left(\cot\left(\frac{1}{2}\sqrt{-\kappa}\zeta\right)\right)^2\right)}{q + \sqrt{-\kappa}\cot\left(\frac{1}{2}\sqrt{-\kappa}\zeta\right)} - k_1 p\left(-\frac{1}{2}\frac{q}{r} - \frac{1}{2}\frac{\sqrt{-\kappa}\cot\left(\frac{1}{2}\sqrt{-\kappa}\zeta\right)}{r}\right)^{-1}, \tag{3.33}$$

$$\begin{aligned} v_{3,3}(x,y,t) = &-\frac{k_1\kappa\left(1 + \sin\left(\sqrt{-\kappa}\zeta\right)\right)}{\cos\left(\sqrt{-\kappa}\zeta\right)\left(-q\cos\left(\sqrt{-\kappa}\zeta\right) + \sqrt{-\kappa}\sin\left(\sqrt{-\kappa}\zeta\right) + \sqrt{-\kappa}\right)} \\ &- k_1 p\left(-\frac{1}{2}\frac{q}{r} + \frac{1}{2}\frac{\sqrt{-\kappa}\left(\tan\left(\sqrt{-\kappa}\zeta\right) + \sec\left(\sqrt{-\kappa}\zeta\right)\right)}{r}\right)^{-1} - \frac{1}{2}k_1 q, \end{aligned} \tag{3.34}$$

and

$$\begin{aligned} v_{3,4}(x,y,t) = &\frac{k_1\kappa\left(\sin\left(\sqrt{-\kappa}\zeta\right) - 1\right)}{\cos\left(\sqrt{-\kappa}\zeta\right)\left(-q\cos\left(\sqrt{-\kappa}\zeta\right) + \sqrt{-\kappa}\sin\left(\sqrt{-\kappa}\zeta\right) - \sqrt{-\kappa}\right)} \\ &- k_1 p\left(-\frac{1}{2}\frac{q}{r} + \frac{1}{2}\frac{\sqrt{-\kappa}\left(\tan\left(\sqrt{-\kappa}\zeta\right) - \sec\left(\sqrt{-\kappa}\zeta\right)\right)}{r}\right)^{-1} - \frac{1}{2}k_1 q. \end{aligned} \tag{3.35}$$

Set. 3.2. With $\kappa > 0,\ r \neq 0$,

$$v_{3,5}(x,y,t) = -\frac{1}{2}k_1 q - \frac{1}{2}\frac{k_1\kappa\left(-1 + \left(\tanh\left(\frac{1}{2}\sqrt{\kappa}\zeta\right)\right)^2\right)}{q + \sqrt{\kappa}\tanh\left(\frac{1}{2}\sqrt{\kappa}\zeta\right)} - k_1 p\left(-\frac{1}{2}\frac{q}{r} - \frac{1}{2}\frac{\sqrt{\kappa}\tanh\left(\frac{1}{2}\sqrt{\kappa}\zeta\right)}{r}\right)^{-1}, \tag{3.36}$$

$$
\begin{aligned}
v_{3,6}(x,y,t) = &-\frac{k_1\kappa\left(-1+i\sinh\left(\sqrt{\kappa}\zeta\right)\right)}{\cosh\left(\sqrt{\kappa}\zeta\right)\left(q\cosh\left(\sqrt{\kappa}\zeta\right)+\sqrt{\kappa}\sinh\left(\sqrt{\kappa}\zeta\right)+i\sqrt{\kappa}\right)}\\
&-k_1p\left(-\frac{1}{2}\frac{q}{r}-\frac{1}{2}\frac{\sqrt{\kappa}\left(\tanh\left(\sqrt{\kappa}\zeta\right)+i\,\mathrm{sech}\left(\sqrt{\kappa}\zeta\right)\right)}{r}\right)^{-1}-\frac{1}{2}k_1q,
\end{aligned}
\tag{3.37}
$$

$$
\begin{aligned}
v_{3,7}(x,y,t) = &-\frac{k_1\kappa\left(1+i\sinh\left(\sqrt{\kappa}\zeta\right)\right)}{\cosh\left(\sqrt{\kappa}\zeta\right)\left(-q\cosh\left(\sqrt{\kappa}\zeta\right)-\sqrt{\kappa}\sinh\left(\sqrt{\kappa}\zeta\right)+i\sqrt{\kappa}\right)}\\
&-k_1p\left(-\frac{1}{2}\frac{q}{r}-\frac{1}{2}\frac{\sqrt{\kappa}\left(\tanh\left(\sqrt{\kappa}\zeta\right)-i\,\mathrm{sech}\left(\sqrt{\kappa}\zeta\right)\right)}{r}\right)^{-1}-\frac{1}{2}k_1q,
\end{aligned}
\tag{3.38}
$$

and

$$
\begin{aligned}
v_{3,8}(x,y,t) = &-\frac{1}{4}\frac{k_1\kappa\left(2\left(\cosh\left(\frac{1}{4}\sqrt{\kappa}\zeta\right)\right)^2-1\right)}{\cosh\left(\frac{1}{4}\sqrt{\kappa}\zeta\right)\sinh\left(\frac{1}{4}\sqrt{\kappa}\zeta\right)\left(-2\,q\cosh\left(\frac{1}{4}\sqrt{\kappa}\zeta\right)\sinh\left(\frac{1}{4}\sqrt{\kappa}\zeta\right)+\sqrt{\kappa}\right)}\\
&-k_1p\left(-\frac{1}{2}\frac{q}{r}-\frac{1}{4}\frac{\sqrt{\kappa}\left(\tanh\left(\frac{1}{4}\sqrt{\kappa}\zeta\right)-\coth\left(\frac{1}{4}\sqrt{\kappa}\zeta\right)\right)}{r}\right)^{-1}-\frac{1}{2}k_1q.
\end{aligned}
\tag{3.39}
$$

Set. 3.3. With $q=\Upsilon$, $p=h\Upsilon(h\neq 0)$ and $r=0$,

$$
v_{3,9}(x,y,t) = -\frac{1}{2}k_1\Upsilon+\frac{k_1\Upsilon\,\mathrm{e}^{\Upsilon\zeta}}{\mathrm{e}^{\Upsilon\zeta}-h}-\frac{k_1h\Upsilon}{\mathrm{e}^{\Upsilon\zeta}-h}.
\tag{3.40}
$$

Set. 3.4. With $q=\Upsilon$, $r=h\Upsilon(h\neq 0)$ and $p=0$,

$$
v_{3,10}(x,y,t) = -\frac{1}{2}k_1\Upsilon-\frac{k_1\Upsilon}{-1+h\mathrm{e}^{\Upsilon\zeta}}.
\tag{3.41}
$$

Set. 3.5. With $p=0$, $r\neq 0$ and $q\neq 0$,

$$
v_{3,11}(x,y,t) = -\frac{1}{2}k_1q+\frac{k_1q\left(\sinh\left(q\zeta\right)-\cosh\left(q\zeta\right)\right)}{-\cosh\left(q\zeta\right)+\sinh\left(q\zeta\right)-\lambda},
\tag{3.42}
$$

and

$$
v_{3,12}(x,y,t) = -\frac{1}{2}k_1q+\frac{k_1q\mu}{\cosh\left(q\zeta\right)+\sinh\left(q\zeta\right)+\mu}.
\tag{3.43}
$$

In above solutions $\zeta=x+y-\omega t$.

4. Graphical discussion

We present depictions for the numerous wave forms found in the framework pursuant to assessment in this part of the paper. We compiled and graphically displayed waves such as dark solitary, bright,

dark-bright, lump-like, dark, anti, and cuspon kinks in 2D, 3D, and contour modes through RMESEM. The results obtained are essential for interpreting the manner in which attributed physical phenomena operate. The objectives of the produced soliton solutions are to significantly expand our comprehension with regard to the theory of long waves with finite amplitude and the related field. Additionally, it has been graphically demonstrated that the solitons in the context of GZK-BBME take the shapes of kink solitons prominently.

Peculiar wave solutions in NPDEs with a supple, resilient, confined transition across the two asymptotic shifts are known as kink solitons. Such waves are seen in some NPDEs, including the GZK-BBME, which models wave propagation in a range of physical systems, including fluids and plasma.

Kink solitons are put into many groups according to the characteristics they exhibit, such as dark, lump-like, cuspon kink, dark-kink, grey kink, and dark-bright kink solitons. In contrast, bright kinks are concentrated, steady wave packets with an energy peak or accumulation that maintains its peak shape and dimension through transmission. Dark-bright kink solitons bring together the properties of both dark wave and bright kinks. Lump-like kinks display locally lump-shaped forms; during propagation, they can alter structure or orientation. Erratic, cusp-type field discontinuities separate cuspon kinks from smoother solitons. Lastly, A grey kink, which produces a waveform with a steeper amplification plunge compared to a black kink, is referred to as a confined, uniform transition with a non-zero deviance distinguishing two hyperbole phases. Being that they preserve their initial configuration as they propagate through the GZK-BBME, kink solitons are important for studying long-wave dispersal amplitude that is finite. Kink solitons persistence occurrence in a variety of media, such as water, provides insight into wave conduct, surf-to-wave interaction, and patterning integrity throughout time and space. Because kink solitons are stable, confined waves that transmit without altering form, they are useful for explaining fluid dynamics, nonlinear wave theory, and plasma physics scenarios. In particular, kink solitons may be used to describe ion-acoustic waveforms in polarized plasmas in plasma physics. Shallow waves of water influenced by both dispersive and nonlinear factors are described by them in fluid dynamics. Furthermore, they are perfect for researching the transmission of energy and communication in nonlinear optical systems and other dispersive media controlled by comparable dynamical equations due to their stability and durability. As demonstrated in this study, these applications highlight the significance of investigating their many forms and behaviors. This information is essential for describing & predicting wave motion in dynamics of fluids, plasma physics, and related purposes.

Remark 1: Figure 1 is plotted for $v_{1,6}$ given in (3.13), which displays an anti-kink soliton profile.

Remark 2: Figure 2 is plotted for $v_{1,9}$ given in (3.16), which displays an anti-kink soliton profile.

Remark 3: Figure 3 is plotted for $v_{2,5}$ given in (3.21), which displays an anti-kink soliton profile.

Remark 4: Figure 4 is plotted for $v_{2,8}$ given in (3.24), the profile shows a bright kink soliton.

Remark 5: Figure 5 is plotted for $v_{2,9}$ given in (3.25), the profile shows a lump-like kink soliton.

Remark 6: Figure 6 is plotted for $v_{2,10}$ given in (3.26), the profile shows a lump-like kink soliton.

Remark 7: Figure 7 is plotted for $v_{2,12}$ given in (3.28), the profile shows a cuspon anti-kink soliton.

Remark 8: Figure 8 is plotted for $v_{3,1}$ given in (3.32), the profile shows a bright-dark kink soliton.

Remark 9: Figure 9 is plotted for $v_{3,5}$ given in (3.36), the profile shows a grey kink soliton.

Remark 10: Figure 10 is plotted for $v_{3,10}$ given in (3.41), the profile shows a solitary kink soliton.

Remark 11: Figure 11 is plotted for $v_{3,12}$ given in (3.43), the profile shows a solitary kink soliton.

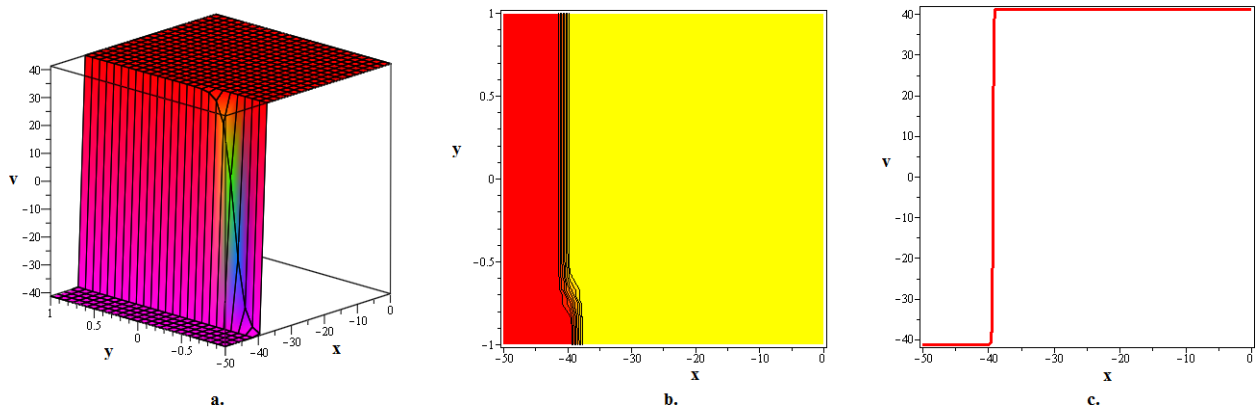

Figure 1. The real part of anti-kink soliton solution $v_{1,6}$, as described in (3.13), is represented in three dimension, with contours and in two dimension ($y = -1$) for the following values of $p := 1; q := 10; r := 8; \omega := -20; s_0 := 10; t := 2$.

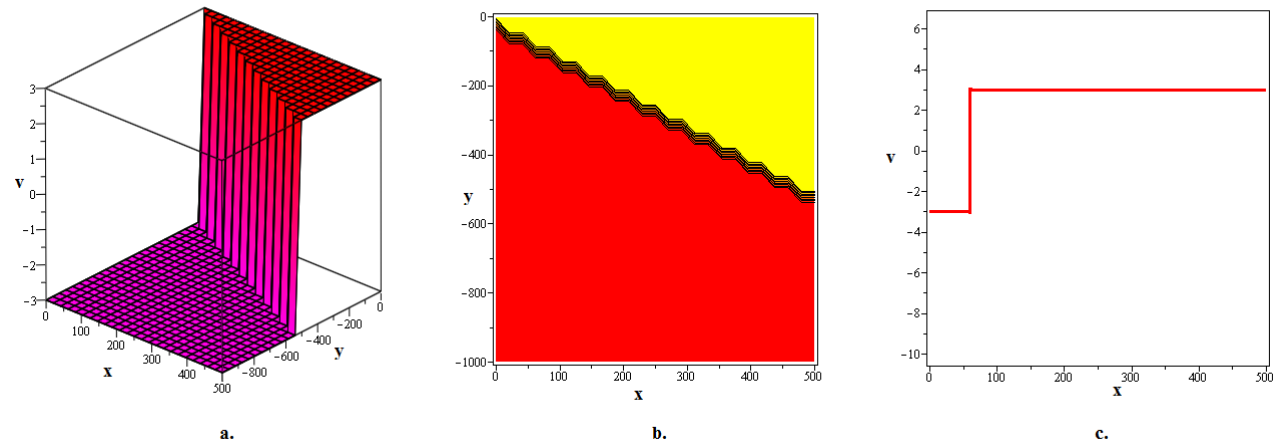

Figure 2. The anti-kink soliton solution $v_{1,9}$, as described in (3.16), is represented in three dimension, with contours and in two dimension ($y = -100$) for the following values of $p := 25; q := 5; h := 5; \Upsilon := 5; r := 0; \omega := -10; s_0 := 30; t := 4$.

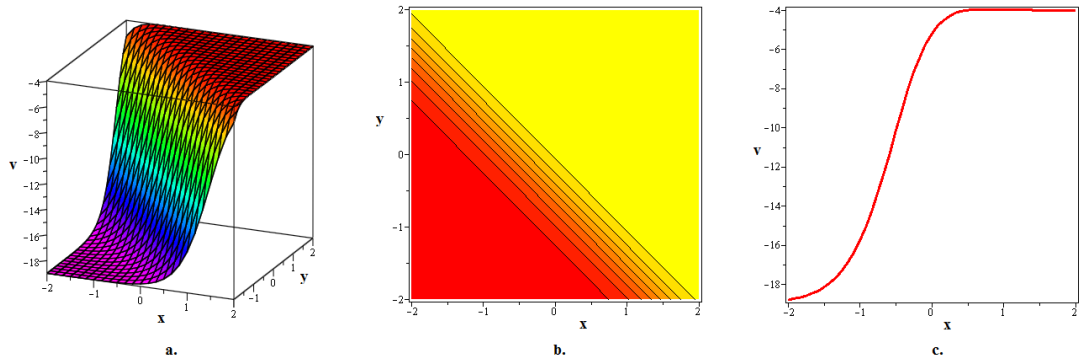

Figure 3. The anti-kink soliton solution $v_{2,5}$, as described in (3.21), is represented in three dimension, with contours and in two dimension ($y = 0$) for the following values of $p := 1; q := 5; r := 4; \omega := 1; k_0 := 1; k_1 := 2; s_0 := 5; t := 0$.

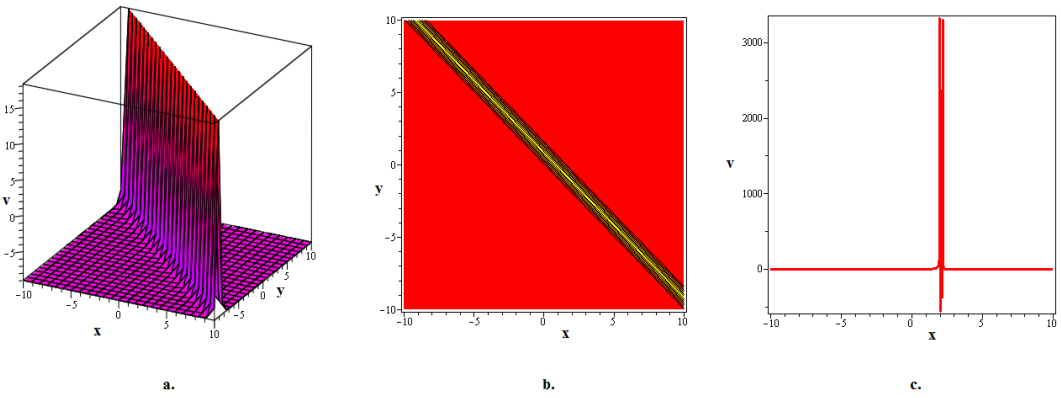

Figure 4. The bright kink soliton solution (also known as a hump kink) $v_{2,8}$, as described in (3.24), is represented in three dimension, with contours and in two dimension ($y = -1$) for the following values of $p := 4; q := 10; r := 4; \omega := 1; k_0 := 3; k_1 := 6; s_0 := 15; t := 1$.

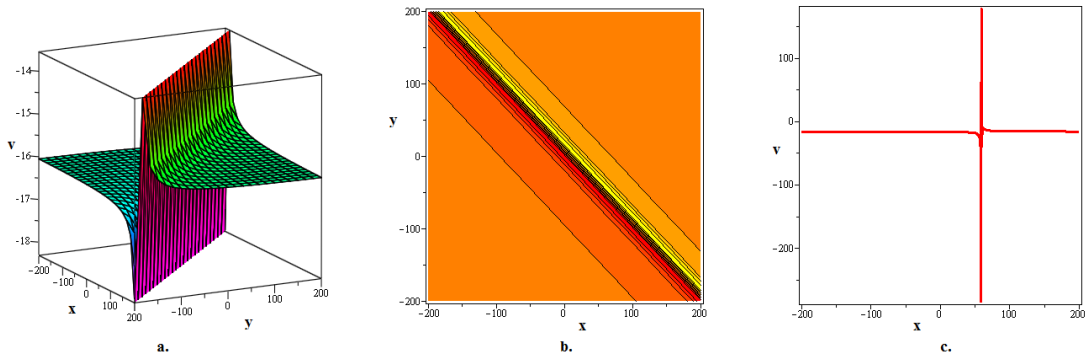

Figure 5. The lump-type kink soliton solution $v_{2,9}$, as described in (3.25), is represented in three dimension, with contours and in two dimension ($y = -50$) for the following values of $p := 1; q := 2; r := 1; \omega := 1; k_0 := 4; k_1 := 8; s_0 := 20; t := 10$.

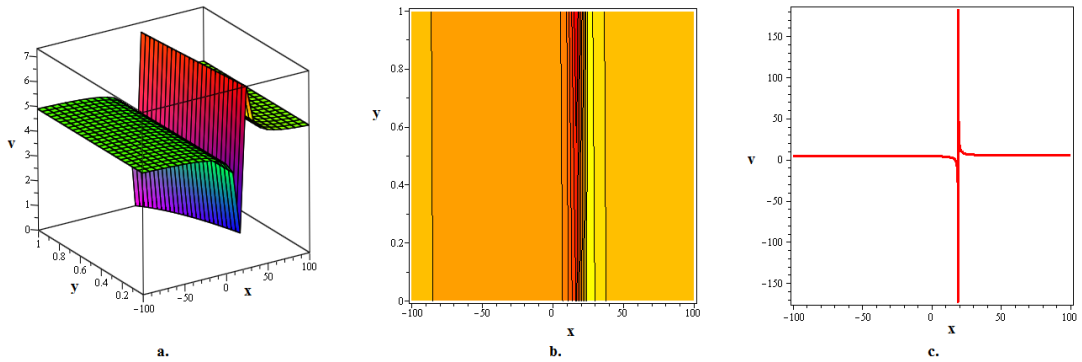

Figure 6. The lump-type kink soliton solution $v_{2,10}$, as described in (3.26), is represented in three dimension, with contours and in two dimension ($y = 1$) for the following values of $p := 15; q := 0; r := 0; \omega := 1; k_0 := 5; k_1 := 10; s_0 := 25; t := 20$.

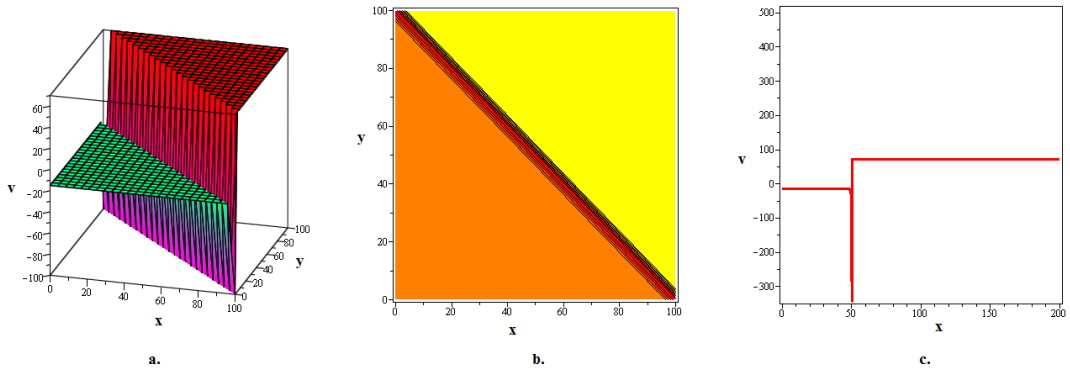

Figure 7. The cuspon anti-kink soliton solution $v_{2,12}$, as described in (3.28), is represented in three dimension, with contours and in two dimension ($y = 50$) for the following values of $p := 6; q := 3; h := 2; \Upsilon := 3; r := 0; \omega := 1; k_0 := 10; k_1 := 20; s_0 := 50; t := 100$.

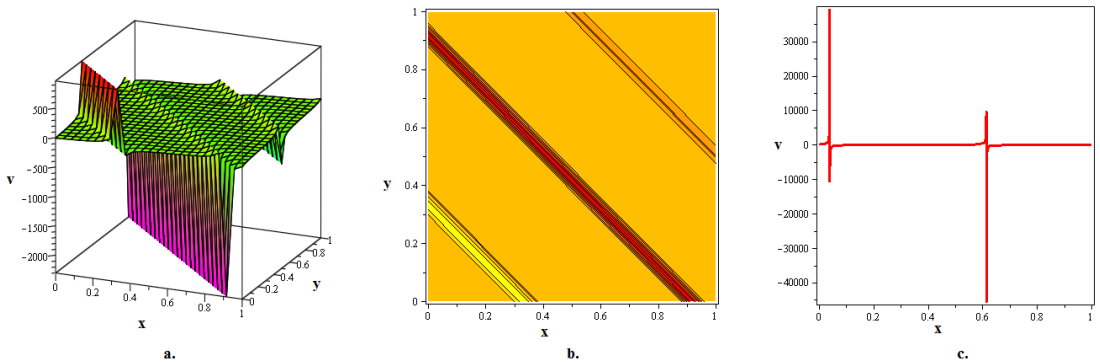

Figure 8. The bright-dark kink soliton solution $v_{3,1}$, as described in (3.32), is represented in three dimension, with contours and in two dimension ($y = 0.3$) for the following values of $p := 6; q := 1; r := 5; \omega := 10; k_0 := 1; k_1 := 5; s_0 := 50; t := 50$.

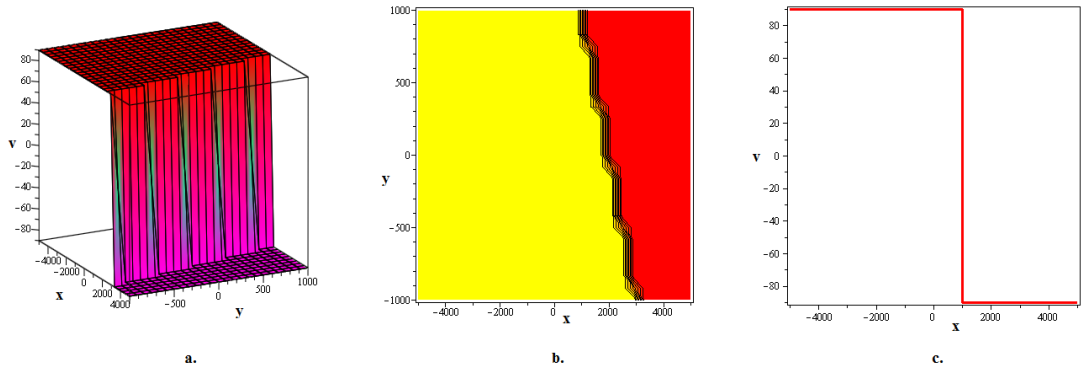

Figure 9. The gray kink soliton solution $v_{3,5}$, as described in (3.36), is represented in three dimension, with contours and in two dimension ($y = 1000$) for the following values of $p := 4; q := 10; r := 4; \omega := 20; k_1 := 30; t := 100$.

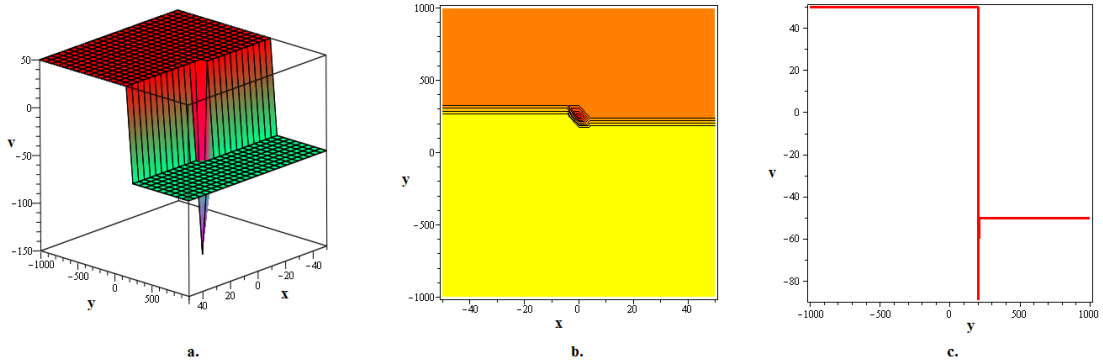

Figure 10. The solitary kink soliton solution $v_{3,10}$, as described in (3.41), is represented in three dimension, with contours and in two dimension ($y = 45$) for the following values of $p := 0; q := 10; r := 20; \Upsilon := 10; h := 2; \omega := 5; k_1 := 10; t := 50$.

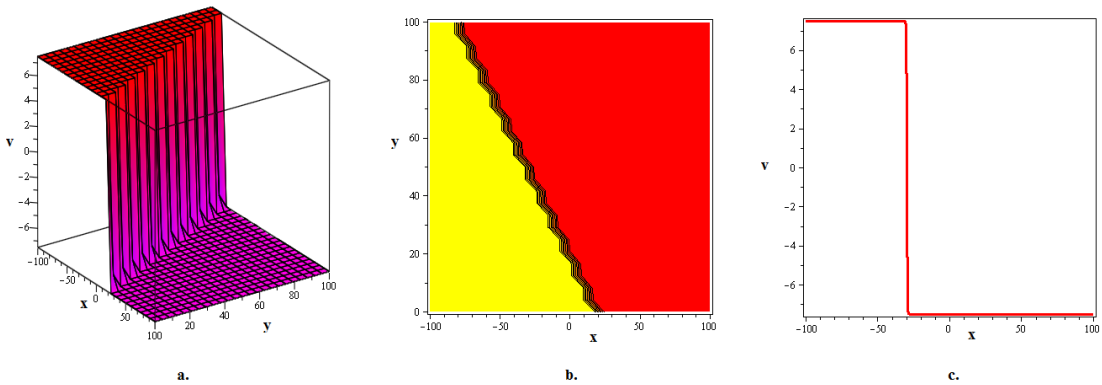

Figure 11. The solitary kink soliton solution $v_{3,12}$, as described in (3.43), is represented in three dimension, with contours and in two dimension ($y = 50$) for the following values of $p := 0; q := 5; r := 5; \omega := 1; k_0 := 2; k_1 := 3; s_0 := 5; t := 20; \mu := 5$.

5. Conclusions

The modernized RMESEM was established in this research to address a nonlinear model, namely GZK-BBME. With the help of the Riccati equation, the RMESEM was capable of arriving at a close form solution for the NODE that the model generated. The propagating soliton solutions that are significant to the problem's physical interpretation were subsequently obtained by shaping this solution into a system of nonlinear algebraic equations. It was shown that different travelling solitons, including dark-kink, lump-type, dark-bright, grey kink, and cuspon kink solitons, exist in kink soliton solutions by presenting multiple 3D, 2D, and contour graphs. The research highlights the implications for several practical applications in the linked fields of nonlinear GZK-BBME and demonstrates how the RMESEM may be utilized to build arrays of soliton solutions for difficult problems, particularly plasma physics and fluid dynamics. Thus, despite the fact that the analysis within the framework of the GZK-BBME provides insight into soliton dynamics that relate to the models of interest, it is constructive to also point out the drawbacks of using this method, especially when the largest derivative and nonlinear term are not equivalent. However, this limitation does not detract from the present study since this work clearly shows that the strategy used in this work is highly efficient, portable, and reliable for nonlinear problems of various natural science disciplines.

Appendix

Some of the above mentioned analytical methods rely on the Riccati equation. These methods are convenient to analyze soliton effects in nonlinear models since the equation of the Riccati type possesses solitary solutions [47]. Based on these applications of the Riccati hypothesis, the current study employed the Riccati equation comprising RMESEM [48] to generate and simulate soliton dynamics in GZK-BBME. This addition was useful as it generated five new families of kink soliton solutions for the targeted model: rational, hyperbolic, periodic, exponential and rational-hyperbolic. From the solutions obtained, significant progress was made towards the understanding of soliton behaviour and establishing a linkage between the events in the targeted model and the mentioned theories. Limiting our method's solutions results in some other strategies' solutions. The analogy is given in the part that follows:

Comparison with other analytical techniques

The outcomes of the other analytical techniques can be obtained using our procedure. As an instance:

Axiom 6.1.1. The following develops after $k_1 = 0$ is configured in (3.4):

$$V(\zeta) = d_0\left(\frac{1}{\Phi(\zeta)}\right). \tag{A.1}$$

This shows that the closed-type result is associated with EDAM. Thus, attaining $k_1 = 0$, our solutions can likewise lead to the results generated by EDAM.

Axiom 6.1.2. Similarly, the following develops after $s_0 = 0$ is configured in (3.4):

$$V(\zeta) = \sum_{j=0}^{1} C_j \left(\frac{\Phi'(\zeta)}{\Phi(\zeta)} \right)^j, \tag{A.2}$$

This is the closed form solution obtained is applying the Riccati equation in the (G'/G)-expansion approach.

As a result, the results of our study might potentially provide a wider range of results generated by the EDAM and (G'/G)-expansion techniques.

Author contributions

N.M.A.A.; Conceptualization, H.Z.; formal analysis, H.Z.; investigation, N.M.A.A.; validation, H.Z.; visualization, N.M.A.A. and H.Z. funding; H.Z.; Data curation, H.Z.; resources, H.Z.; validation, N.M.A.A.; software, H.Z.; resources, N.M.A.A.; project administration, H.Z. writing-review & editing. All authors contributed equally. All authors have read and agreed to the published version of the manuscript.

Use of Generative-AI tools declaration

The authors declare they have not used Artificial Intelligence (AI) tools in the creation of this article.

Conflict of interest

The authors declare that they have no conflicts of interest.

References

1. J. G. Caputo, D. Dutykh, Nonlinear waves in networks: model reduction for the sine-Gordon equation, *Phys. Rev. E*, **90** (2014), 022912. https://doi.org/10.1103/PhysRevE.90.022912
2. X. Yang, Z. Wang, Z. Zhang, Generation of anomalously scattered lumps via lump chains degeneration within the Melnikov equation, *Nonlinear Dyn.*, **111** (2023), 15293–15307. https://doi.org/10.1007/s11071-023-08615-3
3. D. Dutykh, J. G. Caputo, Wave dynamics on networks: method and application to the sine-Gordon equation, *Appl. Numer. Math.*, **131** (2018), 54–71. https://doi.org/10.1016/j.apnum.2018.03.010
4. X. Yang, Z. Wang, Z. Zhang, Decay mode ripple waves within the (3+1)-dimensional Kadomtsev-Petviashvili equation, *Math. Methods Appl. Sci.*, **47** (2024), 10444–10461. https://doi.org/10.1002/mma.10132
5. X. Yang, Z. Wang, Z. Zhang, Solitons and lump waves to the elliptic cylindrical Kadomtsev-Petviashvili equation, *Commun. Nonlinear Sci. Numer. Simul.*, **131** (2024), 107837. https://doi.org/10.1016/j.cnsns.2024.107837
6. R. Ali, Z. Zhang, H. Ahmad, Exploring soliton solutions in nonlinear spatiotemporal fractional quantum mechanics equations: an analytical study, *Opt. Quant. Electron.*, **56** (2024), 838. https://doi.org/10.1007/s11082-024-06370-2

7. R. Ali, E. Tag-eldin, A comparative analysis of generalized and extended $(\frac{G'}{G})$-expansion methods for travelling wave solutions of fractional Maccari's system with complex structure, *Alex. Eng. J.*, **79** (2023), 508–530. https://doi.org/10.1016/j.aej.2023.08.007
8. D. Dutykh, T. Katsaounis, D. Mitsotakis, Finite volume methods for unidirectional dispersive wave models, *Int. J. Numer. Meth. Fluids*, **71** (2013), 717–736. https://doi.org/10.1002/fld.3681
9. D. Dutykh, M. Chhay, F. Fedele, Geometric numerical schemes for the KdV equation, *Comput. Math. Math. Phys.*, **53** (2013), 221–236. https://doi.org/10.1134/S0965542513020103
10. H. Yasmin, A. S. Alshehry, A. H. Ganie, A. M. Mahnashi, R. Shah, Perturbed Gerdjikov-Ivanov equation: soliton solutions via Backlund transformation, *Optik*, **298** (2024), 171576. https://doi.org/10.1016/j.ijleo.2023.171576
11. Y. Kai, Z. Yin, On the Gaussian traveling wave solution to a special kind of Schrödinger equation with logarithmic nonlinearity, *Mod. Phys. Lett. B*, **36** (2021), 2150543. https://doi.org/10.1142/S0217984921505436
12. Y. Kai, Z. Yin, Linear structure and soliton molecules of Sharma-Tasso-Olver-Burgers equation, *Phys. Lett. A*, **452** (2022), 128430. https://doi.org/10.1016/j.physleta.2022.128430
13. C. Zhu, S. A. Idris, M. E. M. Abdalla, S. Rezapour, S. Shateyi, B. Gunay, Analytical study of nonlinear models using a modified Schrödinger's equation and logarithmic transformation, *Results Phys.*, **55** (2023), 107183. https://doi.org/10.1016/j.rinp.2023.107183
14. C. Zhu, M. Al-Dossari, S. Rezapour, S. Shateyi, B. Gunay, Analytical optical solutions to the nonlinear Zakharov system via logarithmic transformation, *Results Phys.*, **56** (2024), 107298. https://doi.org/10.1016/j.rinp.2023.107298
15. S. Guo, A. Das, Cohomology and deformations of generalized Reynolds operators on Leibniz algebras, *Rocky Mountain J. Math.*, **54** (2024), 161–178. https://doi.org/10.1216/rmj.2024.54.161
16. T. A. A. Ali, Z. Xiao, H. Jiang, B. Li, A class of digital integrators based on trigonometric quadrature rules, *IEEE Trans. Ind. Electron.*, **71** (2024), 6128–6138. https://doi.org/10.1109/TIE.2023.3290247
17. K. J. Wang, F. Shi, J. H. Liu, J. Si, Application of the extended F-expansion method for solving the fractional Gardner equation with conformable fractional derivative, *Fractals*, **30** (2022), 2250139. https://doi.org/10.1142/S0218348X22501390
18. F. Wang, M. M. A. Khater, Computational simulation and nonlinear vibration motions of isolated waves localized in small part of space, *J. Ocean Eng. Sci.*, 2022. https://doi.org/10.1016/j.joes.2022.03.009
19. J. Liu, F. Wang, R. A. Attia, S. H. Alfalqi, J. F. Alzaidi, M. M. Khater, Innovative insights into wave phenomena: computational exploration of nonlinear complex fractional generalized-Zakharov system, *Qual. Theory Dyn. Syst.*, **23** (2024), 170. https://doi.org/10.1007/s12346-024-01023-x
20. H. Khan, Shoaib, D. Baleanu, P. Kumam, J. F. Al-Zaidy, Families of travelling waves solutions for fractional-order extended shallow water wave equations, using an innovative analytical method, *IEEE Access*, **7** (2019), 107523–107532. https://doi.org/10.1109/ACCESS.2019.2933188
21. R. Qahiti, N. M. A. Alsafri, H. Zogan, A. A. Faqihi, Kink soliton solution of integrable Kairat-X equation via two integration algorithms, *AIMS Math.*, **9** (2024), 30153–30173. https://doi.org/10.3934/math.20241456

22. H. Khan, S. Barak, P. Kumam, M. Arif, Analytical solutions of fractional Klein-Gordon and gas dynamics equations, via the $(\frac{G'}{G})$-expansion method, *Symmetry*, **11** (2019), 566. https://doi.org/10.3390/sym11040566
23. H. Khan, R. Shah, J. F. Gómez-Aguilar, D. Baleanu, P. Kumam, Travelling waves solution for fractional-order biological population model, *Math. Model. Nat. Phenom.*, **16** (2021), 32. https://doi.org/10.1051/mmnp/2021016
24. J. H. He, X. H. Wu, Exp-function method for nonlinear wave equations, *Chaos Soliton. Fract.*, **30** (2006), 700–708. https://doi.org/10.1016/j.chaos.2006.03.020
25. L. Akinyemi, M. Şenol, O. S. Iyiola, Exact solutions of the generalized multidimensional mathematical physics models via sub-equation method, *Math. Comput. Simul.*, **182** (2021), 211–233. https://doi.org/10.1016/j.matcom.2020.10.017
26. E. Fan, Y. C. Hona, Generalized tanh method extended to special types of nonlinear equations, *Z. Naturforsch. A*, **57** (2002), 692–700. https://doi.org/10.1515/zna-2002-0809
27. S. Kaewta, S. Sirisubtawee, S. Koonprasert, S. Sungnul, Applications of the $(\frac{G'}{G^2})$-expansion method for solving certain nonlinear conformable evolution equations, *Fractal Fract.*, **5** (2021), 88. https://doi.org/10.3390/fractalfract5030088
28. J. Hietarinta, Introduction to the Hirota bilinear method, In: Y. Kosmann-Schwarzbach, B. Grammaticos, K. M. Tamizhmani, *Integrability of nonlinear systems*, Lecture Notes in Physics, Berlin: Springer, **495** (1997), 95–103. https://doi.org/10.1007/BFb0113694
29. M. A. Akbar, L. Akinyemi, S. W. Yao, A. Jhangeer, H. Rezazadeh, M. M. Khater, et al., Soliton solutions to the Boussinesq equation through sine-Gordon method and Kudryashov method, *Results Phys.*, **25** (2021), 104228. https://doi.org/10.1016/j.rinp.2021.104228
30. S. Dai, Poincare-Lighthill-Kuo method and symbolic computation, *Appl. Math. Mech.*, **22** (2001), 261–269. https://doi.org/10.1007/BF02437964
31. S. Akcagil, T. Aydemir, A new application of the unified method, *New Trends Math. Sci.*, **6** (2018), 185–199. https://doi.org/10.20852/ntmsci.2018.261
32. X. F. Yang, Z. C. Deng, Y. Wei, A Riccati-Bernoulli sub-ODE method for nonlinear partial differential equations and its application, *Adv. Differ. Equ.*, **2015** (2015), 117. https://doi.org/10.1186/s13662-015-0452-4
33. I. Ullah, K. Shah, T. Abdeljawad, Study of traveling soliton and fronts phenomena in fractional Kolmogorov-Petrovskii-Piskunov equation, *Phys. Scr.*, **99** (2024), 055259. https://doi.org/10.1088/1402-4896/ad3c7e
34. S. Noor, A. S. Alshehry, A. Shafee, R. Shah, Families of propagating soliton solutions for (3+1)-fractional Wazwaz-BenjaminBona-Mahony equation through a novel modification of modified extended direct algebraic method, *Phys. Scr.*, **99** (2024), 045230. https://doi.org/10.1088/1402-4896/ad23b0
35. H. Yasmin, N. H. Aljahdaly, A. M. Saeed, R. Shah, Probing families of optical soliton solutions in fractional perturbed Radhakrishnan-Kundu-Lakshmanan model with improved versions of extended direct algebraic method, *Fractal Fract.*, **7** (2023), 512. https://doi.org/10.3390/fractalfract7070512
36. H. Yasmin, A. S. Alshehry, A. H. Ganie, A. Shafee, R. Shah, Noise effect on soliton phenomena in fractional stochastic Kraenkel-Manna-Merle system arising in ferromagnetic materials, *Sci. Rep.*, **14** (2024), 1810. https://doi.org/10.1038/s41598-024-52211-3

37. S. A. El-Tantawy, H. A. Alyousef, R. T. Matoog, R. Shah, On the optical soliton solutions to the fractional complex structured (1+1)-dimensional perturbed gerdjikov-ivanov equation, *Phys. Scr.*, **99** (2024), 035249. https://doi.org/10.1088/1402-4896/ad241b
38. M. A. Abdou, A generalized auxiliary equation method and its applications, *Nonlinear Dyn.*, **52** (2008), 95–102. https://doi.org/10.1007/s11071-007-9261-y
39. A. J. M. Jawad, M. D. Petkovi, A. Biswas, Modified simple equation method for nonlinear evolution equations, *Appl. Math. Comput.*, **217** (2010), 869–877. https://doi.org/10.1016/j.amc.2010.06.030
40. W. Hamali, H. Zogan, A. A. Altherwi, Dark and bright hump solitons in the realm of the quintic Benney-Lin equation governing a liquid film, *AIMS Math.*, **9** (2024), 29167–29196. https://doi.org/10.3934/math.20241414
41. T. B. Benjamin, J. L. Bona, J. J. Mahony, Model equations for long waves in nonlinear dispersive systems, *Philos. Trans. Roy. Soc. A*, **272** (1972), 47–78. https://doi.org/10.1098/rsta.1972.0032
42. V. E. Zakharov, E. A. Kuznetsov, Three-dimensional solitons, *Zh. Eksp. Teor. Fiz.*, **66** (1974), 594–597.
43. A. M. Wazwaz, Compact and noncompact physical structures for the ZK-BM equation, *Appl. Math. Comput.*, **169** (2005), 713–725. https://doi.org/10.1016/j.amc.2004.09.062
44. A. M. Wazwaz, The tanh method and the sine-osine method for solving the KP-MEW equation, *Int. J. Comput. Math.*, **82** (2005), 235–246. https://doi.org/10.1080/00207160412331296706
45. K. Khan, M. A. Akbar, N. H. M. Ali, The modified simple equation method for exact and solitary wave solutions of nonlinear evolution equation: the GZK-BBM equation and right-handed noncommutative Burgers equations, *Int. Scholarly Res. Not.*, **2013** (2013), 146704. https://doi.org/10.1155/2013/146704
46. Ö. Güner, A. Bekir, L. Moraru, A. Biswas, Bright and dark soliton solutions of the generalized Zakharov-Kuznetsov-Benjamin-Bona-Mahony nonlinear evolution equation, *Proc. Rom. Acad. Ser. A*, **16** (2015), 422–429.
47. Z. Navickas, R. Marcinkevicius, I. Telksniene, T. Telksnys, M. Ragulskis, Structural stability of the hepatitis C model with the proliferation of infected and uninfected hepatocytes, *Math. Comput. Model. Dyn. Syst.*, **30** (2024), 51–72. https://doi.org/10.1080/13873954.2024.2304808
48. Y. Xiao, S. Barak, M. Hleili, K. Shah, Exploring the dynamical behaviour of optical solitons in integrable kairat-II and kairat-X equations, *Phys. Scr.*, **99** (2024), 095261. https://doi.org/10.1088/1402-4896/ad6e34

AIMS Press